Published by Oxford University Press Human Molecular Genetics, 2002, Vol. 11, No. 12 1439–1447

Neurofilament accumulation at the motor endplate and lack of axonal sprouting in a spinal muscular atrophy mouse model

Carmen Cifuentes-Diaz, Sophie Nicole, Maria E. Velasco, Christophe Borra-Cebrian, Cristina Panozzo, Tony Frugier, Gaelle Millet, Natacha Roblot, Vandana Joshi and Judith Melki*

Molecular Neurogenetics Laboratory, Institut National de la Santé et de la Recherche Médicale (INSERM), Université d'Evry, EMI-9913, GENOPOLE, 91057 Evry, France

Received February 7, 2002; Revised and Accepted March 27, 2002

Mutations of survival of the motor neuron gene (*SMN1*) are responsible for spinal muscular atrophy (SMA), a common genetic cause of death in childhood. The cellular mechanism by which mutations of *SMN1* are responsible for the selective neuromuscular defect and motor neuron cell degeneration observed in SMA has not been described. We have previously generated mice carrying a homozygous deletion of *Smn* exon 7 directed to neurons. We report here that these mutant mice display a dramatic and progressive loss of motor axons involving both proximal and terminal regions, in agreement with the skeletal muscle denervation process and disease progression. Moreover, we found massive accumulation of neurofilaments, including phosphorylated forms, in terminal axons of the remaining neuromuscular junctions. This aberrant cytoskeletal organization of synaptic terminals was associated with reduction of branched structures of the postsynaptic apparatus and defect of axonal sprouting in mutant mice. Together, these findings may be responsible for severe motor neuron dysfunction, and suggest that loss of motor neuron cell bodies results from a 'dying-back' axonopathy in SMA. *Smn* mutant mice should represent a valuable model for elucidating the pathway linking Smn to cytoskeletal organization.

INTRODUCTION

Spinal muscular atrophy (SMA) is an autosomal recessive neuromuscular disorder that represents a common genetic cause of death in childhood. SMA is characterized by degeneration of motor neurons of the spinal cord associated with muscle paralysis and atrophy. SMA has been subdivided into three clinical groups based on age of onset of symptoms, age at death and the achievement of certain motor milestones (1). The acute form of Werdnig–Hoffmann disease (type I) is characterized by severe, generalized muscle weakness within the first 6 months. Death usually occurs within the first 2 years. Type II children are able to sit, although they cannot walk unaided, and they survive beyond 2 years. In type III SMA (or Kugelberg–Welander disease), patients have proximal muscle weakness, starting after the age of 18 months.

Mutations of survival of the motor neuron gene (SMN or SMN1) are responsible for the three types of SMA (reviewed in 2). Homozygous deletion or conversion events of SMN1 exon 7 are the most frequent mutations found in SMA patients (95%), whereas its copy (SMNc or SMN2) remains present (3). Full-length transcripts are almost exclusively produced by SMN1, while the predominant forms encoded by SMN2 lack exon 7 through an alternative splicing of this exon that results in an unstable protein (3–5). SMN is involved in several processes, including cytoplasmic assembly of spliceosomal U snRNPs, pre-mRNA splicing machinery and transcription (6–8). However, the molecular and cellular mechanisms by which mutations of the SMN1 gene, which encodes a ubiquitous protein, are responsible for a selective neuromuscular system involvement and for a progressive disease leading to a paralytic state remain to be unraveled.

To gain insight into the pathogenesis of SMA, mouse models of SMA have been generated (5,9–11). We have recently generated mice carrying a deletion of Smn exon 7, the most frequent mutation found in SMA patients. Since homozygous Smn exon 7 deletion in all cell types resulted in early embryonic lethality, the deletion was directed to neurons using the Cre–loxP system (9). Neuronal mutant mice exhibit a rapid motor deterioration, leading to complete paralysis and death at

*To whom correspondence should be addressed at: Molecular Neurogenetics Laboratory, INSERM, Université d'Evry, EMI-9913, GENOPOLE, 2 rue Gaston Crémieux, CP5724, 91057 Evry, France. Tel: + 33 1 6087 4552; Fax: + 33 1 6087 4550; Email: j.melki@genopole.inserm.fr

a mean age of 4 weeks (9). They develop neurogenic atrophy of skeletal muscle, a constant feature found in human SMA, although the spinal cord had an apparent normal neuronal density (9).

We report here a progressive and dramatic loss of motor axons contrasting with the mild reduction of motor neuron cell bodies in neuronal mutant mice. In addition, we have found an aberrant cytoskeletal organization of 60% of neuromuscular junctions (NMJ), which are characterized by terminal axons filled with neurofilaments (NF), including phosphorylated forms. Abnormal synaptic terminals were associated with reduction of the postsynaptic region as determined by acetylcholine receptor labeling. These findings may be responsible for defect of axonal growth and plasticity, as suggested by the paucity of terminal arborization and the lack of axonal sprouting found in Smn mutant mice.

RESULTS

Dramatic axonal degeneration in neuronal mutant mice

To elucidate the mechanism underlying neurogenic atrophy of muscle fibers, the number of motor neuron cell bodies with detectable nucleoli was evaluated in the anterior horns of spinal cord from mutant ($Smn^{F7}/Smn^{\Delta 7}$, NSE-Cre^{+}) and control mice. Semithin (1 μm) and serial sections of lumbar spinal cord (L4–L5) were obtained from three 30-day-old animals of each group. To avoid repetitive counting, every 70th section was selected and stained with toluidine blue. We observed a mild but significant reduction of motor neuron cell bodies in 30-day-old mutant mice (624 ± 49) when compared with control mice (886 ± 84: a reduction of 30%; $P < 0.001$; Fig. 1). To determine whether the reduction of motor neuron cell bodies was associated with motor axon loss to the same extent, semithin sections of lumbar ventral roots, which contain myelinated axons arising from the motor neurons of the spinal cord, were examined in the same control and mutant mice. Light-microscopic examination of transverse sections stained with toluidine blue revealed striking loss of myelinated axons in L4 and L5 ventral roots of 30-day-old mutant mice (148 ± 63, $n = 3$: a reduction of 78%) compared with ventral roots of control littermates (671 ± 105, $n = 5$; $P = 0.0003$; Fig. 1). Although myelin sheath examination did not reveal striking abnormalities, degeneration of axons was observed in the mutant ventral roots, as judged by the presence of myelin debris (Fig. 1). To determine whether the loss of motor axons occurred at an early stage of the disease course, the number of myelinated axons was evaluated in L4 and L5 ventral roots of three 15-day-old control and mutant mice. A 49% reduction of motor axons was already observed in mutant mice (265 ± 28, $n = 3$) compared with control (522 ± 43, $n = 3$; $P = 0.001$; Fig. 1). Moreover, comparison of motor axon number from 15- and 30-day-old mutant mice revealed a 44% reduction ($P = 0.04$; Fig. 1). These data show the presence of a dramatic and progressive axonal degenerative process in mutant mice. Importantly, the 78% reduction of motor axon number is much more pronounced than the loss of motor neuron cell bodies (30%) in the same 30-day-old mutant mice. Proximal motor axons are thus more prominently affected by the Smn defect

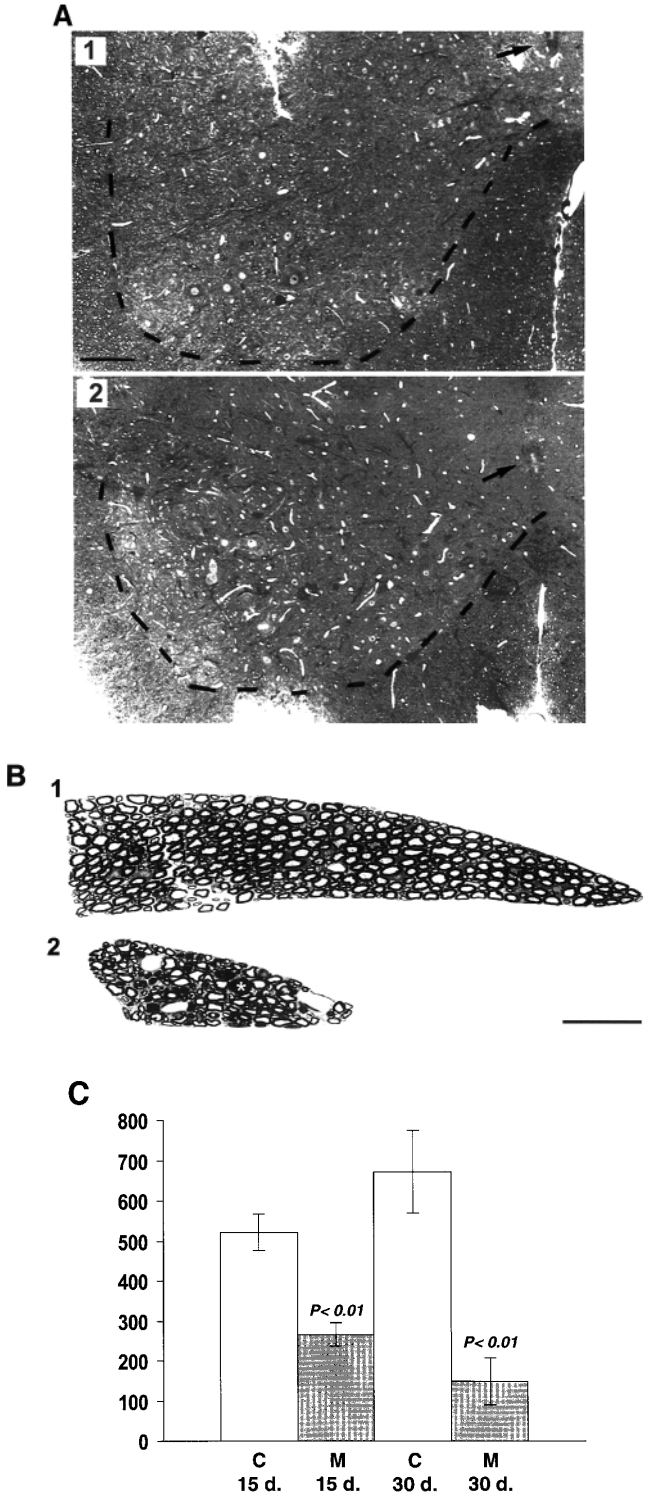

Figure 1. Massive motor axon loss in Smn mutant mice. (A) Moderate loss of motor neuron cell bodies in spinal cord of Smn mutant mice. Semithin sections of ventral horn of lumbar spinal cord from a 30-day-old mutant mouse (1) and an age-matched control mouse (2). Arrow points to ependymal canal. (B) Cross-sections of L5 ventral root from a 30-day-old mutant (2) and a control mouse (1). The asterisk in 2 points to degenerated axon. Sections of 1 μm were stained with toluidine blue. Scale bar = 60 μm (A), 10 μm (B). (C), Total number of myelinated axons in L4 and L5 ventral roots from 30- and 15-day-old mutant (M) and control (C) mice. There is a significant loss of myelinated axons in mutant mice (Student's t-test).

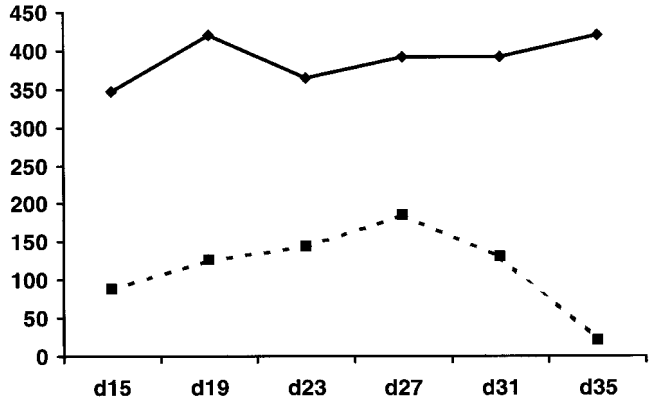

Figure 2. Marked and progressive motor defect of Smn mutant mice. A rotarod test was performed from postnatal day 15 (indicated as d15) every 4 days. Results are presented as time during which mice were able to maintain the rod (given in seconds). Continuous and dashed lines indicate control and mutant mice, respectively.

than are motor neuron cell bodies. In order to evaluate the impact of motor axon loss on motor behavior, a rotarod test was performed. This study included 11 control and 16 mutant mice. The difference between control and mutant mice is significant from 15 days of age in a 5 r.p.m. test ($P < 0.004$, Student's t-test; Fig. 2). The decline in performance of mutant mice was observed at 5 r.p.m. with a biphasic curve: an initial phase (within the first 27 days of age) characterized by a relatively stable deficit, followed by a second phase (starting from 27 days of age) during which the decline was severely progressive, leading to the inability of all mutant mice to maintain their balance for 60 seconds at 5 r.p.m. (Fig. 2).

Massive accumulation of neurofilaments in synaptic terminals of mutant neuromuscular junctions associated with lack of axonal sprouting

To determine whether the degenerative process also involved terminal axons, labeling of NMJ of several skeletal muscles, including extensor digitorum longus (EDL), gastrocnemius, tibialis anterior and sternomastoid muscles, was performed. Whole-mount preparations of teased muscle fibers were stained with rhodamine-conjugated α-bungarotoxin (α-BgTx) and with a monoclonal antibody against the 160 kDa isoform of NF to label the acetylcholine receptor (AChR) and the NF middle subunit (NF-M), respectively. In control animals, NMJ are plaques with branched structures (pretzel-shaped) in which pre- and postsynaptic specializations are closely associated (Figs 3 and 4). In contrast, a lack of terminal axons was observed in some synaptic areas of 30-day-old mutant mice, which further indicates the presence of a muscle denervation process (Fig. 3).

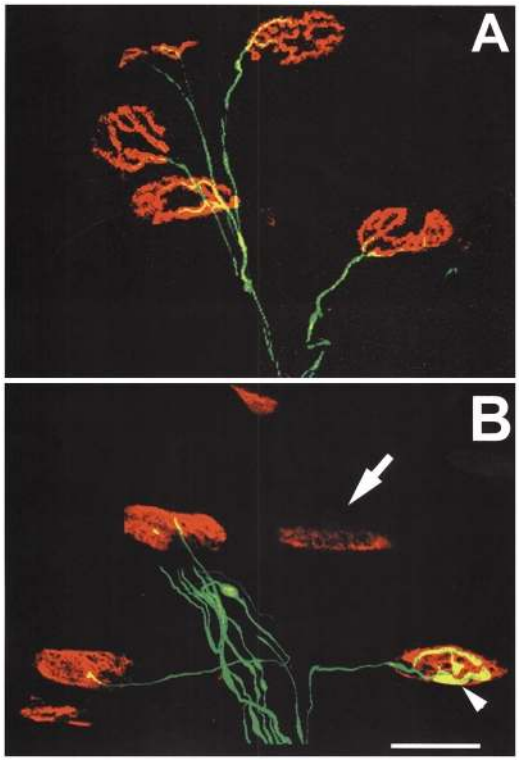

Figure 3. Denervated motor end plates and terminal axons filled with neurofilament (NF) in Smn mutant mice. In toto immunostaining of NMJ on preparations of teased muscle fibers from control (A) and mutant (B) mice. AChR (red) and NF-M (green) labeling revealed denervated NMJ (arrow) or terminal axons filled with NF in mutant mice (arrowhead). Scale bar = 35 μm.

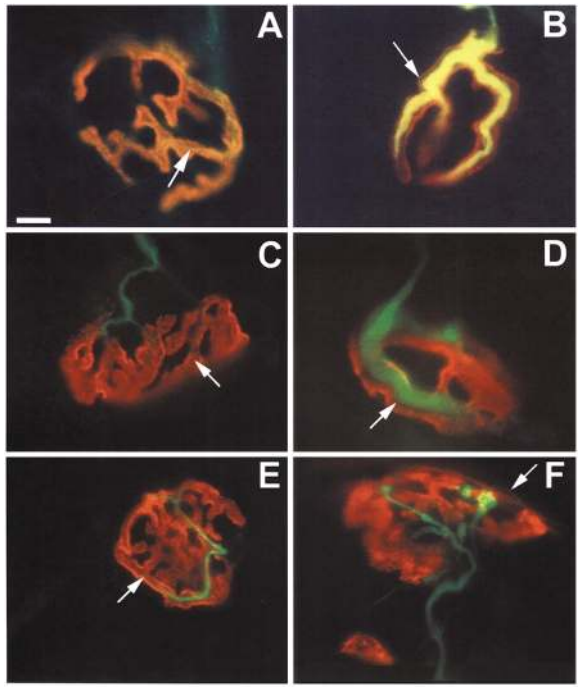

Figure 4. Accumulation of neurofilaments in terminal axons of Smn mutant mice. In toto immunostaining of NMJ of teased muscle fibers from control (A, C) and Smn mutant mice (B, D) of 30-day-old (A, B) and 15-day-old mice (C, D). AChR (red) and NF-M (A, B) or phosphorylated NF-H (C, D, green) labeling revealed terminal axons filled with NF in mutant mice (B, D, arrows). Note the paucity of branched structures of postsynaptic folds in Smn mutant mice (B, D) as determined by AChR labeling when compared with control (A, C). (E, F) In toto immunostaining of NMJ on teased muscle fibers of SOD^{G93A} transgenic mice. Note the thin terminal axons (arrow in E) and the presence of axonal sprouting (arrow in F). Scale bar = 7 μm.

In other synaptic areas, 60% of NMJ (70 out of 119 NMJ) display striking abnormalities, including reduction of branched structures of the subneural apparatus, changes of terminal axons or both (Figs 3 and 4). The postsynaptic surface was evaluated by morphometric analysis of endplates as determined by AChR labeling on teased muscle fibers of control and mutant mice. A significant reduction of postsynaptic areas was observed in 30-day-old mutant (886 ± 88 pixels per endplate, $n = 15$: a reduction of 35%) as compared with control mice (1356 ± 127 pixels per endplate, $n = 15$; $P = 0.005$). Moreover, terminal axons were filled with NF-M as determined by immunolabeling (Figs 3 and 4). Synaptic terminals filled with NF were already present in 15-day-old mutant mice but not in controls of the same age, indicating that this change occurs early in the development of the mutant phenotype (Fig. 4). Surprisingly, no axonal sprouting was detectable in all NMJ examined ($n = 200$). To determine whether the NF accumulation found in synaptic terminals includes phosphorylated forms, SMI-31, a monoclonal antibody specific to phosphorylated NF-H, was used for immunostaining axons in combination with AChR labeling on teased muscle fibers. Terminal axons were filled with phosphorylated NF, indicating the presence of a massive accumulation of phosphorylated NF at the NMJ of mutant mice (Fig. 4).

To determine whether this change was specific to the Smn mutation or caused by a non-specific degenerative process of motor axons, NMJ of paralyzed $SOD1^{G93A}$ transgenic mice (4 months old), a mouse model of amyotrophic lateral sclerosis (ALS), were examined and compared with control mice of the same age (12). No terminal axons filled with NF were observed in the ALS mouse model (Fig. 4). In addition, axonal sprouting associating axonal regeneration and extrajunctional AChR aggregation was easily detectable in the ALS mouse model as previously reported [Fig. 4 and (12)]. These results indicate that terminal axons filled with NF are features specific to the mouse model of SMA.

The presence of terminal axons filled with NF as determined by immunolabeling of NF-M or NF-H suggested that an aberrant cytoskeletal organization of terminal motor axons occurs in Smn mutant mice. Transmission electron-microscopic examination of the NMJ of EDL, gastrocnemius and tibialis anterior was performed in control and mutant mice. In the control mice, there was a high density of synaptic vesicles and mitochondria in the motor nerve terminals associated with folded postsynaptic surface (Fig. 5). In contrast, in the nerve terminals of mutant mice, vesicles were reduced in number. The most striking feature of mutant NMJ was the massive accumulation of NF in synaptic terminals of 13 out of 18 NMJ examined (72%; Fig. 5). Masses of organized or disorganized NF occupied most of the synaptic terminals of mutant mice, whereas NF are absent in the terminal axons of control NMJ (Fig. 5). No microtubule was detected in combination with the abnormal accumulation of NF in mutant terminal axons. The surface of synaptic buttons was evaluated by morphometric analysis of 12 control and mutant NMJ. No significant change was observed, indicating that filling of terminal axons with NF was not associated with oversized terminal axons. In other synaptic areas, postsynaptic folds without apposed terminal axons were observed, which is consistent with the muscle denervation process in mutant mice (Fig. 5). Ultrastructural analysis thus confirmed the presence of abnormal cytoskeletal organization of the terminal motor axons of Smn mutant mice.

Neurofilament accumulation in motor neuron cell bodies and proximal axons

To determine whether NF accumulation was also observed in motor neuron cell bodies of mutant motor neurons, spinal cords from 30-day-old control and mutant mice were processed for both immunofluorescent and electron-microscopic analyses. SMI-31 revealed accumulation of phosphorylated NF-H in numerous large motor neuron cell bodies of mutant mice, whereas in control animals this antibody stained axons only (Fig. 6). Abnormal accumulation of NF in mutant motor neuron perikaryons was further evidenced by immunolabeling of NF-M, whereas perikaryon staining of NF-M was absent in control mice (Fig. 6). Interestingly, the presence of NF accumulation has been detected in motor neuron perikaryons of 15-day-old mutant mice but not in control, indicating that this represents an early change of mutant phenotype (Fig. 6). At the electron-microscopic level, mutant motor neurons displayed eccentrically positioned nuclei associated with indentations of the nuclear membrane, whereas motor neurons of control mice had nuclei in a central position (Fig. 5). At higher magnification, the most striking feature of mutant motor neurons was the abnormal presence of massive bundles of intermediate filaments in the perikaryons and proximal axons (Fig. 5). This contrasts with the normal situation, in which NF are almost undetectable in these cellular compartments, while they are easily detected in the axons (Fig. 5). Immunoblotting experiments were performed to evaluate the expression levels of NF subunits in spinal cord and sciatic nerve of mutant and control mice. Analysis of protein extracts from both tissues revealed no significant change in either size, amount or ratio of NF-M, -H or -L subunits when compared with β-tubulin level (Fig. 7). These results are suggestive of changes in cellular NF distribution rather than deregulation of NF expression. Moreover, the low proportion of motor neurons in the spinal cord and the reduction of motor axons in mutant mice may underestimate the accumulation of NF as determined by both immunofluorescent and electron-microscopic analyses.

NF-H and -M constitute substrates for several protein kinases, including cyclin-dependent kinase 5 (Cdk5). The massive accumulation of phosphorylated forms of NF led us to investigate the cellular distribution and expression of Cdk5 and its neuron-specific regulatory subunit p35 in mutant mice. Immunolabeling and western blot analyses of Cdk5 and p35 revealed no change in either cellular distribution or expression of both proteins in motor neuron cell bodies of mutant mice when compared with control mice (Figs 7 and 8). No accumulation of p25, a truncated form of p35, was observed in spinal cord extracts of mutant mice. In addition to NF-H and -M, the substrates for Cdk5 include the microtubule-associated protein tau. AT8, a monoclonal antibody specific to phosphorylated tau, was used for immunostaining motor neurons of control, SMA and ALS mutant mice. No accumulation of phosphorylated tau was observed in motor neurons of SMA mutant mice, whereas a marked cytoplasmic labeling was observed in motor neuron perikaryons of ALS mutant mice as

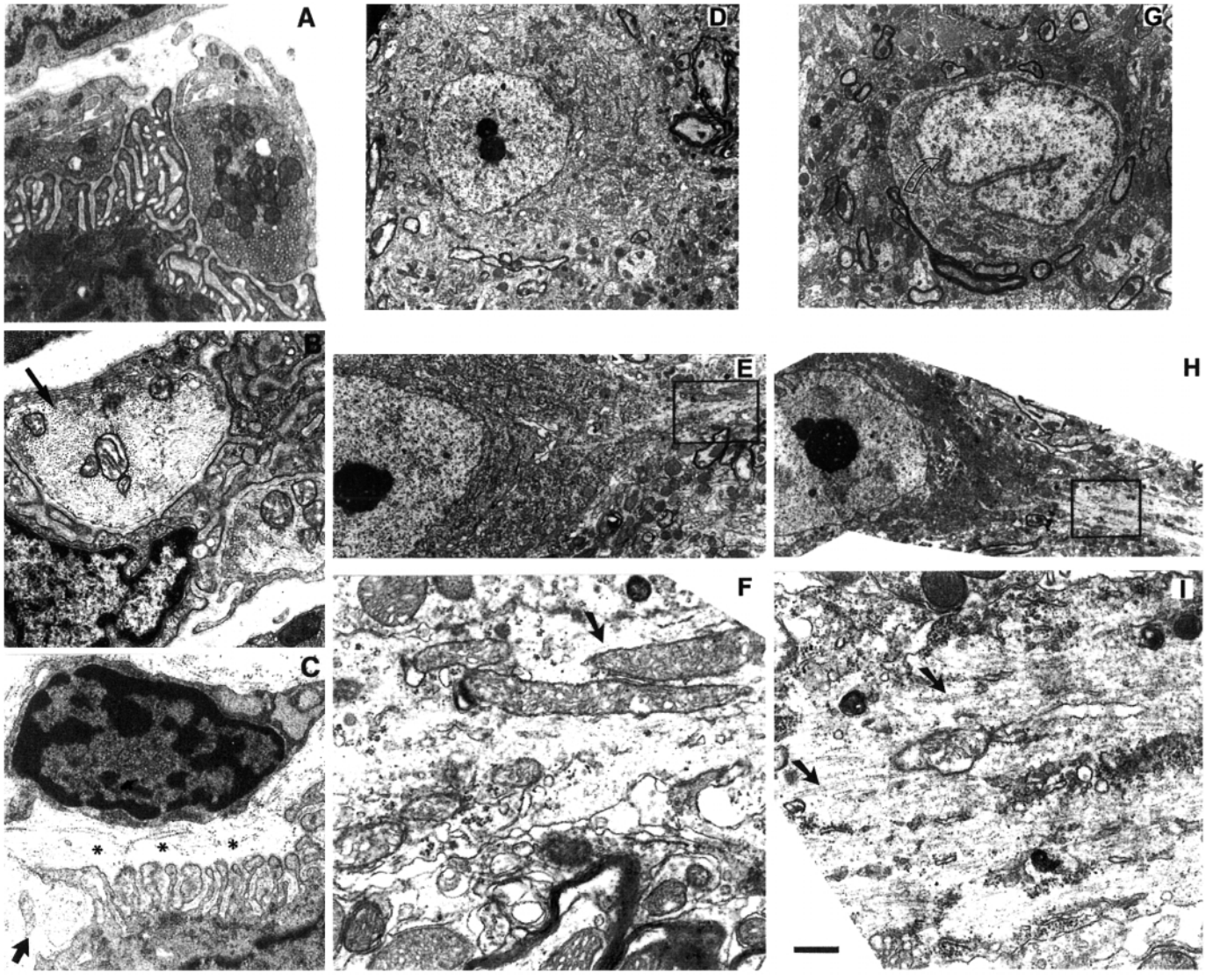

Figure 5. Electron micrographs of NMJ and motor neuron cell bodies of control and mutant mice. Transverse sections of EDL muscle fibers showing the NMJ of control (A) and mutant mice (B, C). Note the absence of terminal axons apposed to postsynaptic folds (asterisks in C) or the massive accumulation of NF in synaptic terminals of mutant mice (arrow in B). Thin sections of motor neuron perikaryons and proximal axons of control (D) and mutant mice (G). The curved arrow in (G) points to the abnormal position of the nucleus associated with indentations of the nuclear membrane. Note the NF accumulation within proximal axons of mutant motor neurons (H, I) (box, arrows) when compared with the same region of control (E, F) (box, arrow). Scale bar = 4 μm (A–C), 10 μm (D, G), 3 μm (E–H), 200 nm (F, I).

previously reported [Fig. 8 and (13)]. These data indicate that the accumulation of phosphorylated NF is neither associated with hyperphosphorylated tau nor caused by deregulation of Cdk5/p35 activity or distribution in SMA mutant mice.

DISCUSSION

We report here the presence of a dramatic and progressive loss of proximal motor axons (up to 78% reduction) which is consistent with the muscle denervation process and the progressive motor deterioration leading to the paralytic state of neuronal mutant mice. In addition, comparison between the loss of motor axons and that of motor neuron cell bodies from the same mutant mice revealed that motor axons are more severely affected by the Smn defect than are motor neuron cell bodies (reductions of 78% and 30%, respectively). To determine whether the degenerative process of motor axons involved terminal regions, labeling of NMJ was performed. Examination of mutant NMJ showed striking abnormalities of terminal axons filled with NF, including phosphorylated forms, associated with reduction of branched structures of the subneural apparatus. Aberrant accumulation of NF in synaptic terminals was further confirmed by ultrastructural analysis of mutant NMJ. Massive accumulation of NF, including phosphorylated forms, was also observed in motor neuron perikaryons and proximal axons, as determined by both immunofluorescent and electron-microscopic analyses. Importantly, accumulation of phosphorylated NF in both perikaryons

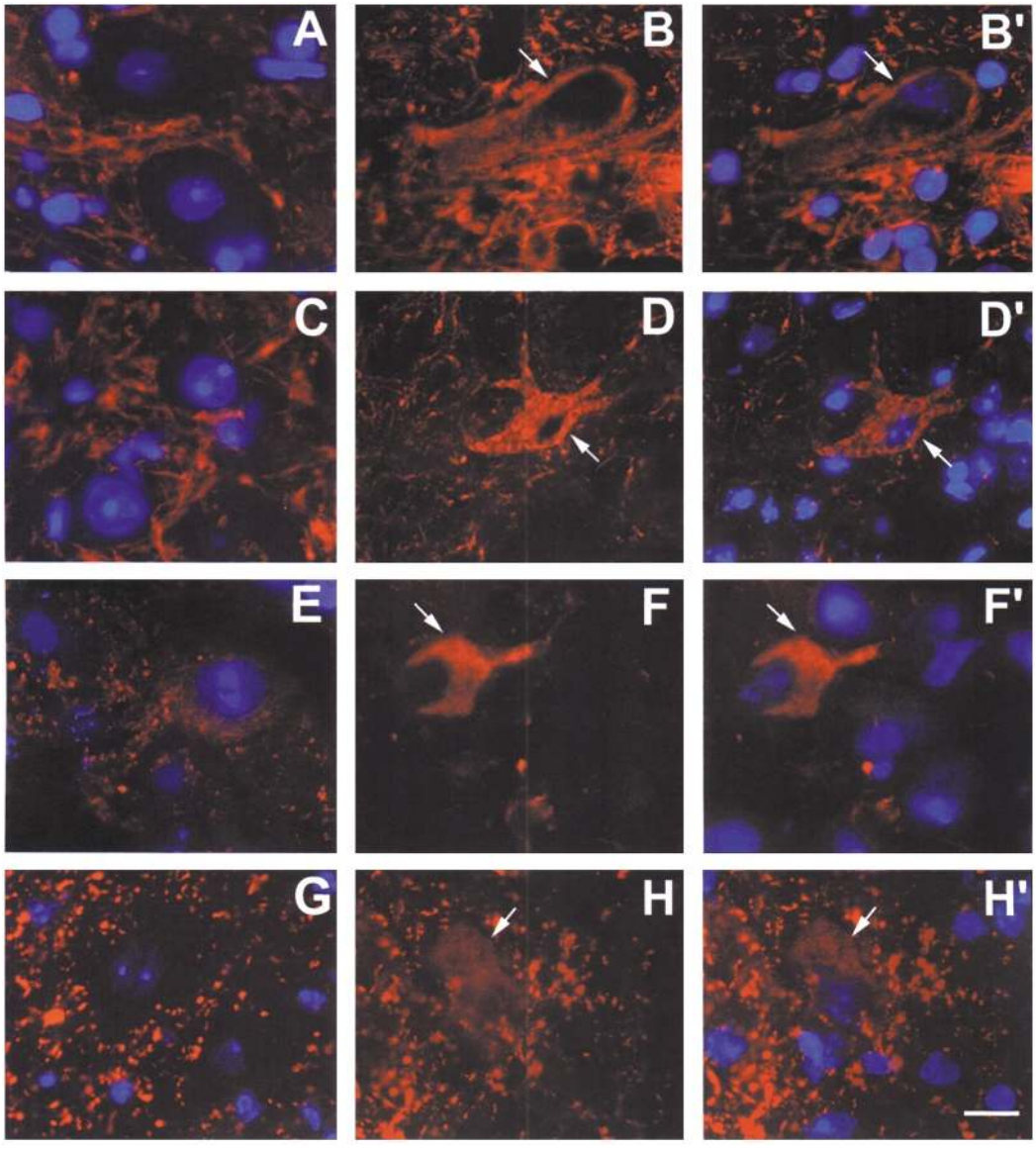

Figure 6. Accumulation of neurofilaments in motor neuron perikaryons of mutant mice. Immunofluorescent labeling experiments of NF-M (A–D′), NF-L (E, F, F′) and NF-H (G, H, H′) on transverse sections of spinal cord from control (A, C, E, G) and mutant (B, B′, D, D′, F, F′, H, H′) mice. Arrows point to NF accumulation in motor neuron perikaryons, shown using monoclonal antibodies against the NF-M, NF-L or the phosphorylated form of NF-H subunits. Note the accumulation of NF-M in motor neuron perikaryons of 15- (B, B′) and 30-day-old mutant mice (D, D′), whereas no labeling was observed in motor neuron perikaryons of control mouse of the same age (A, 15-day-old; C, 30-day-old). Nuclei are stained with DAPI. Scale bar = 20 μm.

and terminal axons has been detected in 15-day-old mutant mice, indicating that it represents an early event in SMA pathogenesis. Surprisingly, no axonal sprouting was detectable in mutant mice, despite the presence of denervated NMJ intermixed with NMJ showing terminal axons filled with NF. These results indicate an abnormal organization of synaptic terminals associated with a defect of axonal regeneration in Smn mutant mice. To determine whether these changes were specific to the Smn defect, NMJ have been studied in paralyzed SOD^{G93A} transgenic mice, a mouse model of ALS characterized by motor neuron degeneration (12). No terminal axons filled with NF and numerous axonal sprouts were observed in the ALS model, indicating that NMJ changes in Smn mutant mice are specific to the Smn defect and are not caused by a non-specific axonal degenerative process.

NF-H and -M constitute substrates for Cdk5 (14). Deregulation of Cdk5 or its neuron-specific regulatory subunit p35 has been reported in several neurodegenerative diseases, including ALS and Alzheimer's disease (13,15). Both NF and the microtubule-associated protein tau, another substrate for Cdk5, have been found to be highly phosphorylated, suggesting that deregulation of Cdk5 or p35 might contribute to pathogenesis of these diseases (13,15). Neither changes in the expression or in cellular distribution of Cdk5 and p35 nor accumulation of highly phosphorylated tau have been found in

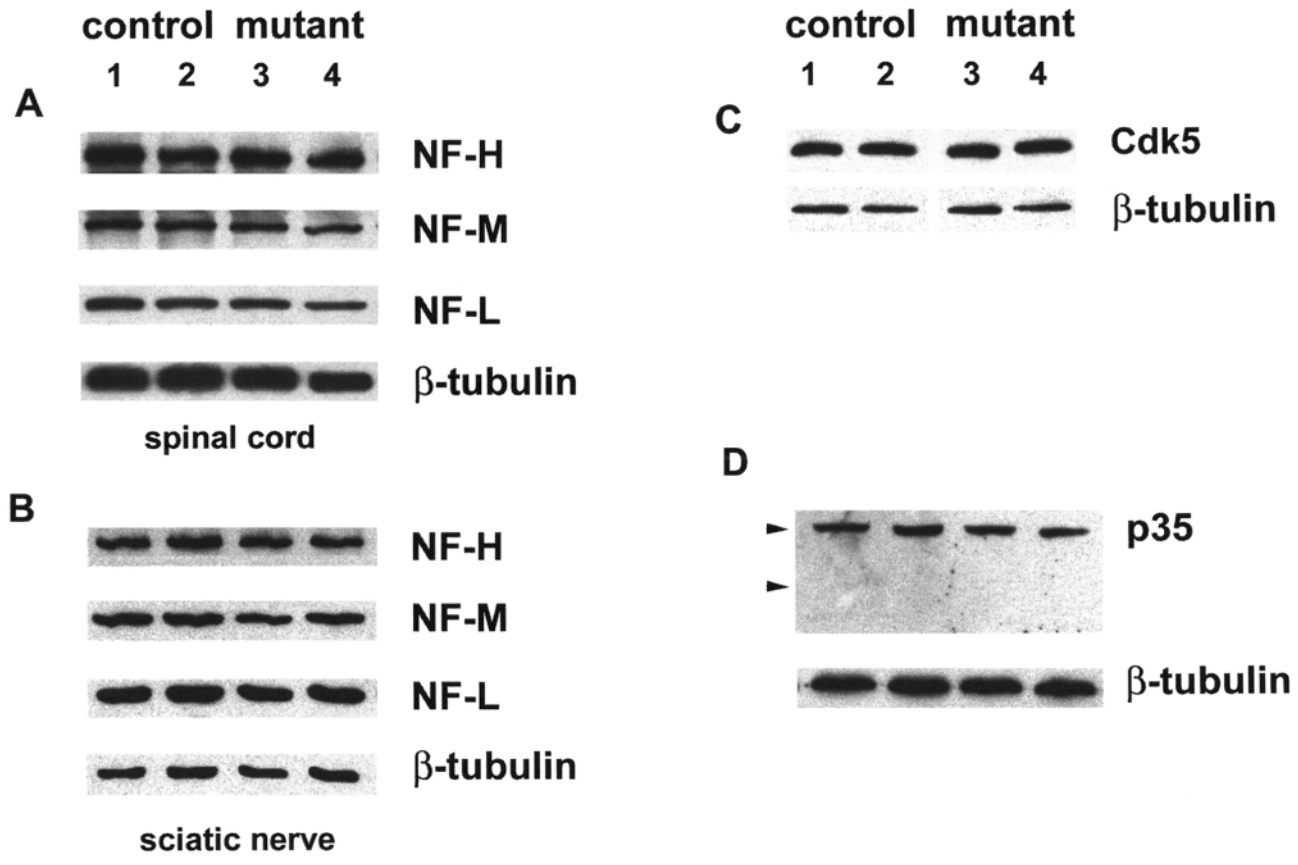

Figure 7. Immunoblotting analysis of neurofilaments, Cdk5 and p35 in Smn mutant mice. Expression level of NF subunits in spinal cord (A) or sciatic nerves (B) of control (lanes 1 and 2) and mutant (lanes 3 and 4) mice. No changes in the amount of NF-H, -M or -L were observed in spinal cord or sciatic nerve extracts from mutant when compared with control mice. Expression levels of Cdk5 (C) and p35 (D) were similar in control (lanes 1 and 2) and mutant (lanes 3 and 4) spinal cord tissues. No accumulation of p25 was observed in spinal cord extracts from Smn mutant mice. Arrows point to the expected sizes of p35 and p25. β-Tubulin was used as internal control.

motor neurons of Smn mutant mice. Our data strongly suggest that accumulation of phosphorylated NF in Smn mutant mice is not caused by deregulation of the Cdk5/p35 complex. Accumulation of NF in perikaryons and proximal axons has been regarded as a by-product of the pathogenic process or even as a protection of neurons from the detrimental hyperphosphorylation of tau in ALS (13). Comparing mouse models of SMA and ALS has revealed (i) massive accumulation of phosphorylated NF in synaptic terminals of motor axons in SMA but not in ALS, (ii) an absence of highly phosphorylated forms of tau in SMA and (iv) normal distribution or expression of Cdk5/p35 in SMA. These data indicate that NF accumulation observed in both mutants results from distinct pathways. Whether the accumulation of NF is a primary effect of the loss of SMN function or a secondary event via an unidentified pathway remains to be investigated.

The neuronal cytoskeleton, including neurofilaments and microtubules, is generated in the neuronal soma and transported along the axons. However, NF are not present in synaptic terminals, and it is thought that NF are degraded by a calcium-activated protease to prevent the accumulation of NF in terminal axons (16,17). Cytoskeletal components play a major role in axonal growth and plasticity (18). Abnormal accumulation of NF in terminal axons of Smn mutant mice may contribute to the defect in terminal axonal growth and plasticity, as suggested by the paucity of terminal arborization, the reduction of branched structures of the subneural apparatus and the defect in axonal sprouting in Smn mutant mice. The resulting aberrant cytoskeletal organization at the NMJ of mutant mice may contribute to the loss of motor neuron function. Moreover, the severe degenerative changes in both proximal and terminal axons contrast with the mild reduction of motor neuron cell bodies. Our data suggest that loss of motor neuron cell bodies may result from a dying-back axonopathy starting from terminal axons.

Skeletal muscle has recently been reported as another tissue targeted by the Smn defect, leading to destabilization of the sarcolemma as determined by marked reduction of dystrophin expression and upregulation of utrophin (5). Both proteins represent key components of skeletal muscle fibers linking the F-actin cytoskeleton to the extracellular matrix. Therefore, an Smn defect directed to either neurons or skeletal muscle leads to destabilization of cytoskeletal components or interacting proteins in targeted tissues. Smn mutant mice should represent valuable models for elucidating the pathway linking SMN to cytoskeletal organization.

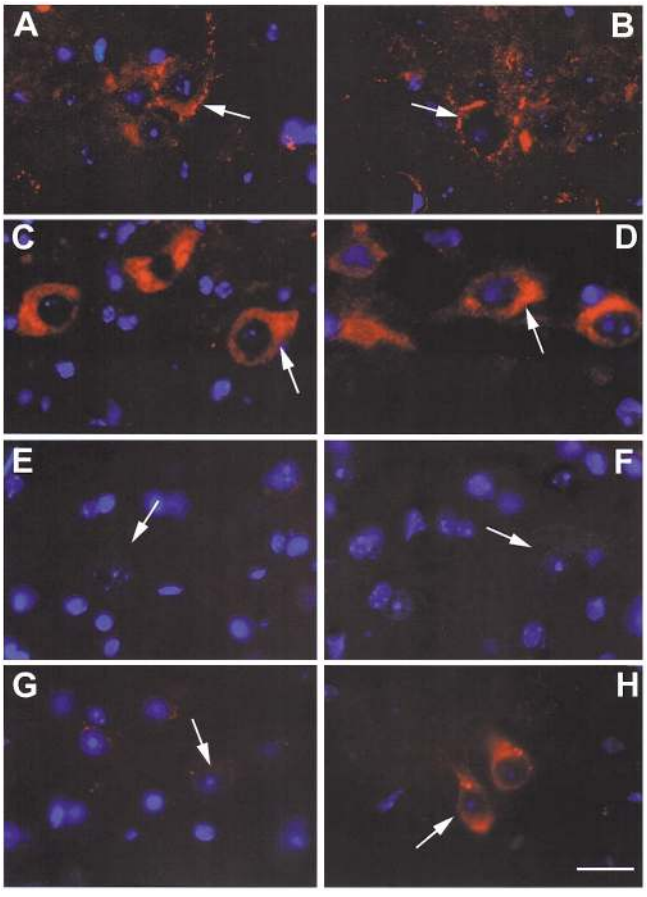

Figure 8. Immunolabeling of Cdk5, p35 and phosphorylated tau in Smn mutant mice. Immunofluorescent labeling experiments on transverse sections of spinal cord from control (A, C, E, G), SMA mutant (B, D, F) and ALS mutant (H) mice. Expression and cellular distribution of Cdk5 (A, B) and p35 (C, D) were similar in control and SMA mutant mice. Immunolabeling experiments of phosphorylated tau in control (E, G), SMA mutant (F) and ALS mutant mice (H). Note the absence of phosphorylated tau labeling in control and SMA mutant mice, whereas massive accumulation was found in perikaryons of ALS mutant motor neurons (arrow in H). Small dots in (G) and (H) are autofluorescent products. Nuclei are stained with DAPI. Scale bar = 20 μm.

MATERIALS AND METHODS

Mice

Mice carrying deletion of Smn exon 7 directed to neurons ($Smn^{F7}/Smn^{\Delta 7}$, NSE-Cre^{+}) were produced as previously described (9). ($Smn^{F7}/+$) animals from the same littermate were used as controls. Transgenic mice expressing $SOD1^{G93A}$ (12) were purchased from Jackson Laboratory and maintained on a C57BL6 genetic background. Animals were genotyped by PCR amplification of DNA extracted from tail biopsies as previously described (9,12). All animal procedures were performed in accordance with institutional guidelines (agreements A91-228-2 and 3429).

Immunofluorescence staining

Transverse frozen sections (10 μm) of lumbar spinal cord were prepared from three 15- or 30-day-old control or mutant mice. Sections were fixed in 2% paraformaldehyde (10 minutes), bathed in PBS (pH 7.4) with 0.1 M glycine (30 minutes) and treated with blocking buffer containing 3% BSA and 0.5% Triton X-100 (10 minutes). Sections were then incubated with monoclonal antibodies against the light subunit of NF (NF-L, NR4; Sigma), the middle subunit (NF-M, NN18; Chemicon Inc., CA) and the heavy subunit (NF-H, SMI-31; Sternberger Monoclonals Inc., Lutherville, MD). For Cdk5 labeling, C-8 rabbit polyclonal antibodies were used (Santa Cruz Biotechnology, Santa Cruz, CA). Immunolabeling of p35 was performed using polyclonal antibodies specific to peptide mapping to the C or N terminus (C-19 or N-20, respectively; Santa Cruz Biotechnology, Santa Cruz, CA). For tau immunolabeling, AT8, a monoclonal antibody specific to phosphorylated forms, was used (Innogenetics, Belgium). Immunolabeling of Cdk5, p35 or tau was performed on transverse sections of spinal cord from perfused mice as previously described (13). Sections were mounted with Vectashield with DAPI (Vector Laboratories, Burlingame, CA) and observed under a Zeiss Axiophot fluorescence microscope.

In toto immunostaining of NMJ of gastrocnemius, tibialis anterior, extensor digitorum longus (EDL) and sternomastoid was performed on particles from three 15- or 30-day-old control or mutant mice as previously described (5). Presynaptic motor nerve terminals were labeled with monoclonal antibody directed against the NF-M (NN18) or NF-H (SMI-31), and AChR was labeled with rhodamine-conjugated α-bungarotoxin (Molecular Probes, Eugene, OR).

Histologic and ultrastructural analysis

Toluidine blue staining of the spinal cord or ventral roots was performed on semithin sections prepared from perfused tissues of three 15- or 30-day-old control or mutant mice as previously described (9,19). Ultrathin sections were obtained from these tissues or skeletal muscle and stained with uranyl acetate and lead citrate for electron-microscopic analysis. Sections were observed at 80 kV and photographed on a Philips CM transmission electron microscope. Morphometric analysis was performed using Duoscan T1200 apparatus and Quantity One software (Biorad, Hercules, CA).

Western blot analysis

Frozen spinal cord or sciatic nerves from three 30-day-old mutant or control mice were crushed in liquid nitrogen using a mortar and pestle. Pulverized tissue samples were transferred to Laemmli buffer supplemented with protease inhibitor cocktail (1 μl/20 mg of wet weight, Sigma, St Louis, MO), 2 mM PMSF and phosphatase inhibitors (20 mM sodium fluoride, 10 mM sodium molybdate and 100 μM sodium orthovanadate). Then the extracts were boiled for 5 minutes. After centrifugation at 11 000 g for 5 minutes, supernatants were collected, electrophoresed on 8% SDS-polyacrylamide gel and electrotransferred to nitrocellulose membranes (Schleicher and Schuell). The membranes were then blocked in 5% non-fat dry milk in TBS 1× and consecutively incubated with monoclonal antibodies (NF-L, NF-M, NF-H or β-tubulin; Chemicon Inc., CA) or polyclonal antibodies against Cdk5 or p35 (C-8 and C-19, respectively). The membranes were washed for 5 minutes in

four changes of TBS 1 × and 0.05% Tween-20 and incubated with anti-mouse or -rabbit IgG conjugated to horseradish peroxidase. The immune complexes were revealed using chemiluminescent detection reagents (Pierce, Rockford, IL).

Rotarod test

Testing was started from 15 days of age, and animals were studied every 4 days. This study included 11 control and 16 mutant mice. The protocol consisted of placing mice on a rod (3.6 cm in diameter) placed 20 cm above the floor of the apparatus and rotating at 5 r.p.m. (Bioseb, Chaville, France). The test was stopped after an arbitrary limit of 7 minutes. For each session, two trials were performed with a resting interval of 1 minute. Results are given as the time the mice were able to maintain their balance on the rod.

ACKNOWLEDGEMENTS

We thank J.P. Denizot and J. Molgo (Institut A. Fessard, CNRS, Gif-sur-Yvette) for sharing equipment for electron-microscopic analysis. This work was supported by INSERM, the Association Française contre les Myopathies (AFM), Families of SMA (USA), Andrew's Buddies (USA), the Fondation pour la Recherche Médicale, Aventis, the Conseil Regional d'Ile de France and GENOPOLE.

REFERENCES

1. Munsat, T.L. (1991) Workshop report: International SMA Collaboration. Neuromusc. Disord., 1, 81.
2. Lefebvre, S., Burglen, L., Frezal, J., Munnich, A. and Melki, J. (1998) The role of the SMN gene in proximal spinal muscular atrophy. Hum. Mol. Genet., 7, 1531–1536.
3. Lefebvre, S., Bürglen, L., Reboullet, S., Clermont, O., Burlet, P., Viollet, L., Benichou, B., Cruaud, C., Millasseau, P., Zeviani, M. et al. (1995) Identification and characterization of a spinal muscular atrophy-determining gene. Cell, 80, 155–165.
4. Lorson, C.L. and Androphy, E.J. (2000) An exonic enhancer is required for inclusion of an essential exon in the SMA-determining gene SMN. Hum. Mol. Genet., 9, 259–265.
5. Cifuentes-Diaz, C., Frugier, T., Tiziano, F.D., Lacene, E., Roblot, N., Joshi, V., Moreau, M.H. and Melki, J. (2001) Deletion of murine SMN exon 7 directed to skeletal muscle leads to severe muscular dystrophy. J. Cell Biol., 152, 1107–1114.
6. Fischer, U., Liu, Q. and Dreyfuss, G. (1997) The SMN–SIP1 complex has an essential role in spliceosomal snRNP biogenesis. Cell, 90, 1023–1029.
7. Pellizzoni, L., Naoyuki, K., Charroux, B. and Dreyfuss, G. (1998) A novel function for SMN, the spinal muscular atrophy disease gene product, in pre-mRNA splicing. Cell, 95, 615–624.
8. Pellizzoni, L., Charroux, B., Rappsilber, J., Mann, M. and Dreyfuss, G. (2001) A functional interaction between the survival motor neuron complex and RNA polymerase II. J. Cell Biol., 152, 75–85.
9. Frugier, T., Tiziano, F.D., Cifuentes-Diaz, C., Miniou, P., Roblot, N., Dierich, A., Le Meur, M. and Melki, J. (2000) Nuclear targeting defect of SMN lacking the C-terminus in a mouse model of spinal muscular atrophy. Hum. Mol. Genet., 9, 849–858.
10. Hsieh-Li, H.M., Chang, J.G., Jong, Y.J., Wu, M.H., Wang, N.M., Tsai, C.H. and Li, H. (2000) A mouse model for spinal muscular atrophy. Nat. Genet.,24, 66–70.
11. Monani, U.R., Sendtner, M., Coovert, D.D., Parons, W.D., Andreassi, C., Le, T.T., Jablonka, S., Schrank, B., Rossol, W., Prior, T.W., Morris, G.E. and Burghes, A.H. (2000) The human centromeric Survival Motor neuron gene (SMN2) rescues embryonic lethality in $SMN^{-/-}$ mice and results in a mouse with spinal muscular atrophy. Hum. Mol. Genet., 9, 333–339.
12. Gurney, M.E., Pu, H., Chiu, A.Y., Dal Canto, M.C., Polchow, C.Y., Alexander, D.D., Caliendo, J., Hentati, A., Kwon, Y.W., Deng, H.X., Chen, W., Zhai, P., Sufit, R.L. and Siddique, T. (1994) Motor neuron degeneration in mice that express a human Cu,Zn superoxide dismutase mutation. Science, 264, 1772–1775.
13. Nguyen, M.D., Lariviere, R.C. and Julien, J.P. (2001) Deregulation of Cdk5 in a mouse model of ALS: toxicity alleviated by perikaryal neurofilament inclusions. Neuron, 30, 135–147.
14. Guidato,S, Tsai L.H., Woodgett, J. and Miller, C.C. (1996) Differential cellular phosphorylation of neurofilament heavy side-arms by glycogen synthase kinase-3 and cyclin-dependent kinase-5. J. Neurochem., 66, 1698–1706.
15. Patrick, G.N., Zukerberg, L., Nikolic, M., de la Monte, S., Dikkes, P. and Tsai, L.H. (1999) Conversion of p35 to p25 deregulates Cdk5 activity and promotes neurodegeneration. Nature, 402, 615–622.
16. Schlaepfer, W.W. (1974) Calcium-induced degeneration of axoplasm in isolated segments of rat peripheral nerve. Brain Res., 69, 203–215.
17. Schlaepfer, W.W. and Micko, S. (1978) Chemical and structural changes of neurofilaments in transected rat sciatic nerve. J. Cell Biol., 78, 369–378.
18. Tanaka, E. and Sabry, J. (1995) Making the connection: cytoskeletal rearrangements during growth cone guidance. Cell, 83, 171–176.
19. Li, M., Sendtner, M., Smith, A. (1995) Essential function of LIF receptor in motor neurons. Nature, 378, 724–727.